Epilepsy Research 161 (2020) 106300

Contents lists available at ScienceDirect

Epilepsy Research

journal homepage: www.elsevier.com/locate/epilepsyres

Assessment of cardiac structure and function in a murine model of temporal lobe epilepsy

Alba González[a,b], Cecilie Gjessing Nome[b], Bård Andre Bendiksen[c,d,e], Ivar Sjaastad[c,d], Lili Zhang[c,d], Mona Aleksandersen[f], Erik Taubøll[a,b], Dag Aurlien[g], Kjell Heuser[a,*]

[a] Dep. of Neurology, Oslo University Hospital, Rikshospitalet, Oslo, Norway
[b] Faculty of Medicine, University of Oslo, Oslo, Norway
[c] Institute for Experimental Medical Research (IEMR), Oslo University Hospital, Ullevål, Oslo, Norway
[d] KG Jebsen Center for Cardiac Research, University of Oslo, Oslo, Norway
[e] Bjørknes University College, Oslo, Norway
[f] School of Veterinary Medicine, Norwegian University of Life Sciences (NMBU), Ås, Norway
[g] Neuroscience Research Group and Dep. of Neurology, Stavanger University Hospital, Stavanger, Norway

ARTICLE INFO

Keywords:
SUDEP
Sudden unexpected death in epilepsy
Cardiac fibrosis
MRI
Murine model
Temporal lobe epilepsy
Intracortical kainate mouse model

ABSTRACT

Sudden unexpected death in epilepsy (SUDEP) is a significant cause of premature seizure-related death. An association between SUDEP and cardiac remodeling has been suggested. However, whether SUDEP is a direct consequence of acute or recurrent seizures is unsettled. The purpose of this study was to evaluate the impact of status epilepticus (SE) and chronic seizures on myocardial structure and function.

We used the intracortical kainate injection model of temporal lobe epilepsy to elicit SE and chronic epilepsy in mice. In total, 24 C57/BL6 mice (13 kainate, 11 sham) were studied 2 and 30 days post-injection. Cardiac structure and function were investigated in-vivo with a 9.4 T MRI, electrocardiography (ECG), echocardiography, and histology [Haematoxylin/Eosin (HE) and Martius Scarlet Blue (MSB)] for staining of collagen proliferation and fibrin accumulation.

In conclusion, we did not detect any significant changes in cardiac structure and function neither in mice 2 days nor 30 days post-injection.

1. Introduction

Sudden unexpected death in epilepsy (SUDEP) is a tragic complication of epilepsy with an estimated incidence rate of 1.2–1.4 per 1000 patient-years (Harden et al., 2017; Saetre and Abdelnoor, 2018). SUDEP is defined as nontraumatic and nondrowning death of a person with epilepsy, without a toxicological or anatomical cause of death detected during the postmortem examination (Nashef et al., 2012).

The pathophysiological mechanisms underlying SUDEP are complex and incompletely understood. Despite increased research on SUDEP over the past years, substantial gaps in knowledge exist.

Suggested pathophysiological mechanisms include seizure-related respiratory failure and cardiac arrhythmias, most probably due to alteration of autonomic function during ictal, postictal, or even interictal states (Isojärvi et al., 1998; Nashef et al., 1996; Myers et al., 2018). A genetic predisposition modifying both the brain and the heart and leading to both epilepsy and cardiac arrhythmias have been proposed (Glasscock et al., 2010; Noebels, 2017). Seizures typically activate the sympathetic nervous system resulting in increased heart rate and blood pressure, but may, on the other hand, via parasympathetic activation or sympathetic inhibition lead to reduced heart and respiratory rates and decreased blood pressure (Devinsky, 2004). The latter may mainly occur when seizures involve the central autonomic network, which frequently follows spreading from the temporal brain region (Tinuper et al., 2001; Ansakorpi et al., 2000, 2002; Suorsa et al., 2011). Besides the direct impact of seizures on autonomic heart function, it is debated whether acute and/or chronic repetitive seizures induce structural damage to the myocardium. Walton and collaborators demonstrated an increase in heart weight in post-status epilepticus rats compared with controls, concluding that this difference was secondary to cardiac structural changes (Walton et al., 1995). Several postmortem investigations of SUDEP patients report perivascular/ interstitial fibrosis and myocyte vacuolization (Earnest et al., 1992; P-Codrea Tigaran et al., 2005). As myocardial fibrosis leads to increased myocardium

* Corresponding author at: Department of Neurology, Oslo University Hospital - Rikshospitalet, PO Box 4950, Nydalen, 0424, Oslo, Norway.
E-mail address: kjell.heuser@ous-hf.no (K. Heuser).

https://doi.org/10.1016/j.eplepsyres.2020.106300
Received 10 October 2019; Received in revised form 28 January 2020; Accepted 22 February 2020
Available online 24 February 2020

stiffness and cellular miscommunication of cardiomyocytes (Istrătoaie et al., 2015; Krenning et al., 2010), the cardiac function could be altered in epilepsy patients and potentially contribute to seizure-related death (P-Codrea Tigaran et al., 2005). This is underpinned by a few animal experiments showing structural changes and cardiomyocyte pathologies like vacuolization, cardiac fibrosis, and inflammatory cell infiltration after chemically induced status epilepticus (SE) (Walton et al., 1995; Read et al., 2015; Auzmendi et al., 2018). However, recent comprehensive and systematic evaluation of earlier post mortem studies of SUDEP patients challenge the concept of structural cardiac damage associated with SUDEP (Nascimento et al., 2017; Devinsky et al., 2018). Our study was motivated by recent experiments performed in adult rats in which the authors combined echocardiography and histology and reported on decreased ejection fraction 48 h and 28 days post SE, as well as dilated cardiomyopathy after 28 days (Read et al., 2015). The aim of our study was to investigate the impact of SE and chronic epilepsy, respectively, on heart structure and function in mice. To our knowledge, this is the first comprehensive study on cardiac function and structure in acquired epilepsy in mice. As epilepsy with temporal origin is frequently associated with SUDEP (Mueller et al., 2014), we used the intracortical kainate injection model of temporal lobe epilepsy as described by Bedner and colleagues (Bedner et al., 2015).

2. Methods

2.1. Animals and study design

A total of 24 male C57BL/6 mice were obtained from JanVier labs (Le Genest-Saint-Isle, France) at eight weeks of age. The animals were hosted 4–5 mice/cage on a regular 12-hrs light/dark cycle at 21 °C room temperature and had free access to water and food. All animals had an acclimatization period of 7 days before experiments were conducted. The use of animals complied with the National Institute of Health Guide for the Care and Use of Laboratory Animals (2011), and permission was granted by the Norwegian Food Safety Authority (project ID 5760).

Once the animals were acclimatized, a baseline recording was performed to obtain data from ECG (n = 24), MRI (n = 10), and echocardiography (n = 24). Fig. 1 shows the schematic diagram of the experimental setup.

Before the operation, animals were divided into two groups: 13 received kainate injection and 11 saline (sham) injection. One sham animal died immediately after the procedure.

After 2 days, all animals were studied with ECG, echocardiography, and MRI. Four sham and 6 kainate injected animals were sacrificed for histological studies. This rendered data available for MR, ECG, and echocardiography for 10 sham and 13 kainate injected animals and histology data available from 4 sham and 6 kainate injected mice.

After 30 days, the remaining 13 mice, 6 sham and 7 kainate were sacrificed. All 13 animals were studied with MRI, ECG, echocardiography, and histology.

2.2. Surgical procedure

We used the intracortical kainate injection mouse model of mesial temporal lobe epilepsy (MTLE), as described by Bedner et al. (Bedner et al., 2015). Mice were anesthetized with a mixture of medetomidine (0.3 mg/kg, i.p.) and ketamine (40 mg/kg, i.p.). Animals were kept on a heating pad during the procedure and until four hours after the injection, maintaining a stable body temperature of around 37 °Celsius.

A small craniotomy was performed by using a stereotactic frame, and kainate (70 nl; 20 mM; Tocris) was injected intracortical above the right hippocampus by using a Hamilton pipette (Hamilton Company, NV) at a depth of 1.7 mm at the following coordinates relative to the bregma: anteroposterior −2.0 mm and lateral +1.5 mm.

Anesthesia was stopped with atipamezole (300 mg/kg, i.p.), and SE was observed clinically.

Control animals were injected with saline, but otherwise treated exactly the same.

As described by Bedner et al., this method reliably elicits SE shortly after the induction which terminates spontaneously after several hours. The animals recover physically within 1–2 days and develop spontaneous seizures after a latent period of median 5 days (Bedner et al., 2015).

2.3. Cardiac MRI

Anesthesia was induced in a chamber containing 3% isoflurane in room air enriched with 50 % pure oxygen. Subsequently mice were placed in an MRI container tube allowing maintenance of continuous flow of adjustable isoflurane and oxygen supply to maintain anesthesia (Fig. 2). MRI recordings were carried out using a 35-mm quadrature-driven birdcage RF coil (Rapid Biomedical, Rimpar, Germany) in a 9,4 T preclinical MRI system (Agilent, Palo Alto, CA, USA). The temperature, heart rate, and respiratory rate were consistently monitored during experiments and kept within the physiological range. Heated air was used to maintain animal body temperature at 37 °Celsius (Fig. 2).

MRI cine data sets were acquired using a motion-compensated gradient echo sequence. Seven to ten ventricular short-axis slices were obtained, covering the heart from base to apex. Central imaging parameters were as follows: echo/repetition time 2.10/4.70 ms; field of view 30 × 30 mm; acquisition matrix 128 × 128 mm; slice thickness 1.00 mm; flip angle 15°; averages 2. For tissue phase mapping (TPM) (Espe et al., 2017a) acquisitions one four-chamber long-axis slice and one mid-ventricular short-axis were acquired using the following parameters: TR 3,41; TE 2,42; field of view 25.6 × 25.6 mm; acquisition matrix 96 × 96 mm; slice thickness 1.0 mm; averages 1. Two flow saturation bands were positioned over the veins to suppress the incoming blood flow. T1 mapping was performed on a four-chamber long axis slice and a mid-ventricular short axis-slice pre- and 30 min post-intraperitoneal (i.p.) injection of 0.5 mmol/kg Gd-DTPA-BMA (Omniscan, GE Healthcare, Hatfield, UK) field of view 25.6 × 25.6 mm; acquisition matrix 128 × 128 mm. All the MRI recordings were both ECG and respiration gated. Total scanning time was approximately 60 min per animal. The operators were blinded to experimental groups. MRI data were analyzed using Image J (General Public License) and MatLab (The MathWorks, Natick, Massachusetts, USA) with the operator blinded to animal groups (Espe et al., 2017b).

2.4. ECG and echocardiography

ECG and echocardiography were performed on all animals using a Vevo2100 system (VisulaSonics Inc) (Finsen et al., 2005). Examinations were executed under light anesthesia with 1.75 % isoflurane in freely breathing animals. After anesthesia, the mice were placed in a physiological monitoring system plate that facilitates the manipulation during the images and allows ECG monitoring. For the latter, the limbs of the animal are fixed at the ends of the monitoring plate through monitoring pads. The pads contain electrodes, and these were connected to the right front paw and the left hind paw and automatically sampled the animal's ECG to the machine.

Echocardiography was conducted with the animal over the monitoring system plate in supine position. An i13 l 13-MHz linear array transducer custom made for mouse imaging was for all recording of data placed in the left parasternal position to obtain two-dimensional (2D) images of: 1) LV in both long and short axes. Short axis recordings were obtained at the level of the papillary muscle, 2) M-mode was acquired at the level of the papillary muscles and the aortic valves, 3) LV wall thickness and diameter dimensions were estimated in diastole and systole through the largest diameter of the ventricle. This procedure is described in detail by Sadredini et al. (Sadredini et al., 2016). As

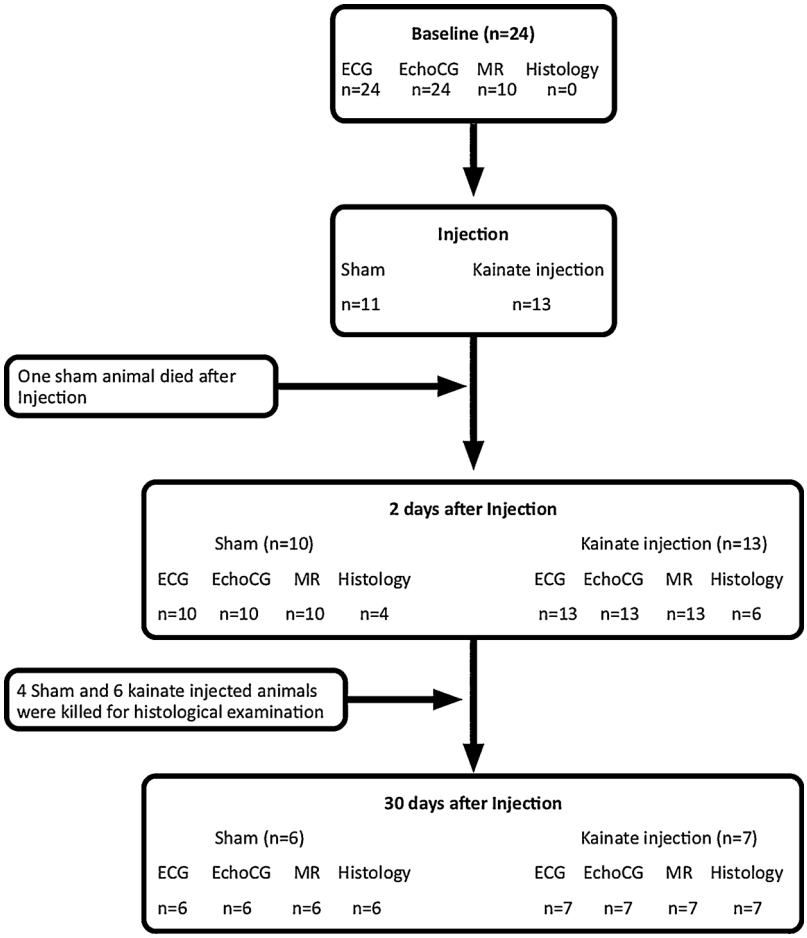

Fig. 1. Overview of the experimental setup.

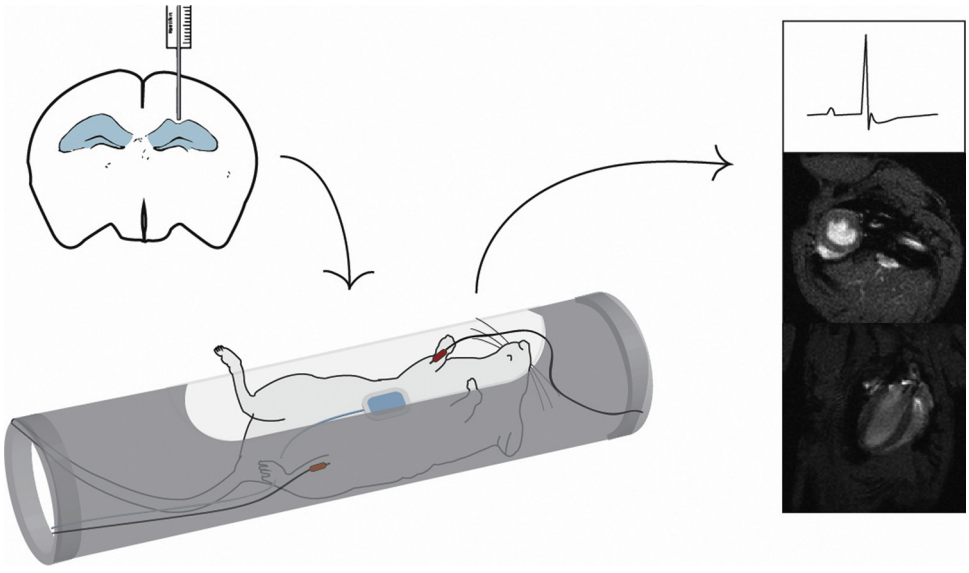

Fig. 2. Illustration of the MRI setup.
Mice were injected with kainate or saline water above the right hippocampus. After two days and 30 days post-injection animals underwent ECG, echocardiography and MRI. The figure illustrates the injection procedure, MRI setup, and ECG.

illustrated by Espe et al. (Espe et al., 2017b) the data were analyzed offline using Image J (General Public License) and MatLab (The MathWorks, Natick, MA), with the operator blinded to animal groups. The procedure is noninvasive, with no discomfort to the animals.

2.5. Histology

All animals were anesthetized with isoflurane and sacrificed to excise the heart. The heart was cut along the septum in two pieces: one half was instantly frozen in nitrogen, the other half was fixed in 4 %

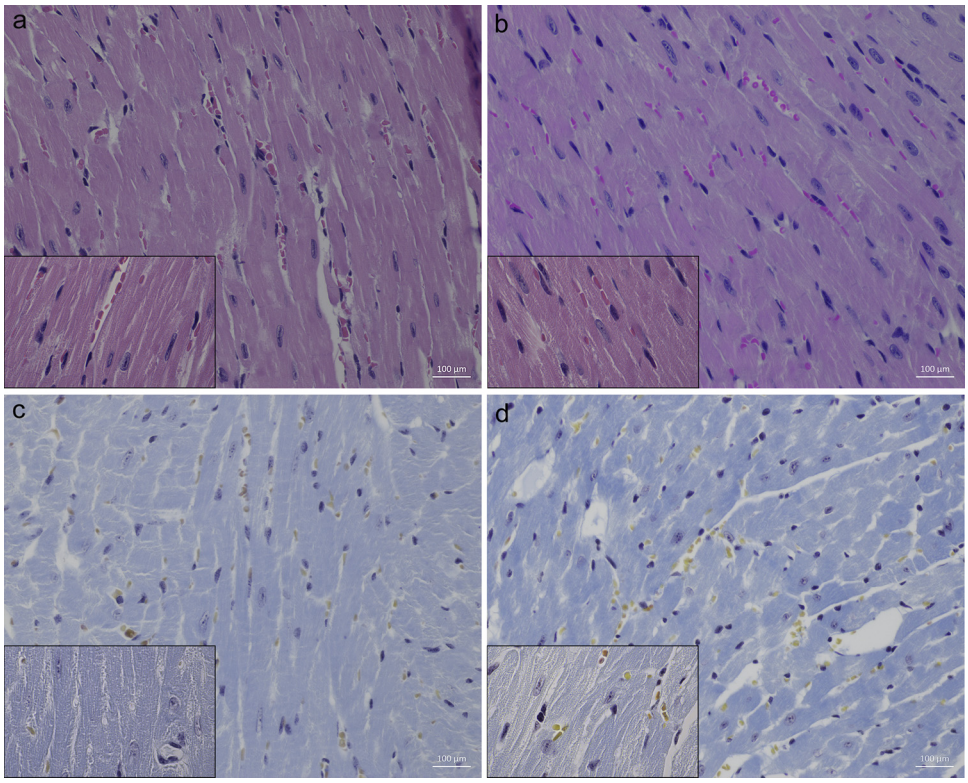

Fig. 3. HE and MSB staining of the mouse heart.
Myocardium of mice 30 days after injection with kainate and sham. a and b: HE stained sections of a kainate injected mouse (a) and a control mouse (b). The myocardium of mice in both groups showed normal histology. *Inset*: Higher magnification of myocardium (1000x). c and d: MSB stained sections of a kainate injected mouse (c) and a control mouse (d). The cardiomyocytes have normal morphology and no proliferation of fibrous tissue is present. *Inset*: Higher magnification of myocardium (1000x).

phosphate buffered formaldehyde for 24 h and then transferred to 70 % ethanol until further processing. Samples were routinely processed and embedded in paraffin. Sections were cut 3 − 4 µm in thickness. We examined three incisions from each heart, two of which were stained with hematoxylin and eosin (HE) and one with Martius Scarlet Blue (MSB) for evaluation of fibroplasia (Fig. 3).

All sections were examined by light microscopy in a blinded manner by a trained pathologist.

The same histological methods applied in this study are frequently used in human tissue samples from post-mortem epilepsy patients to evaluate evaluate structural changes in the myocardium (Natelson et al., 1998; P-Codrea Tigaran et al., 2005; Devinsky et al., 2018; Istrătoaie et al., 2015).

2.6. Statistical analysis

Data management and analysis were performed using SPSS 23.0 (IBM Corp. Released in 2010. IBM SPSS Statistics for Windows, Version 23.0). Data are presented as means with standard deviations (SD). Differences between groups were calculated using Chi-square test and *t*-test where appropriate. A two-sided p-value $\leq$ 0.05 was considered significant.

3. Results

3.1. Seizure observation

The intracortical, juxtahippocampal administration of kainate caused an immediate onset of generalized epileptic seizures in all animals characterized by typical tonic-clonic movements in the upper and lower extremities and tail rectification. Such behavior was never observed in sham animals. Only animals with observed continuous convulsions for > 120 min after kainate injection were included in the study. We also observed spontaneous recurrent seizures in the chronic phase (after 7 days post-injection). Chronic seizures were however not systematically analyzed, as seizure phenotype analysis was not in the scope of this study, and due to lacking compatibility of surveillance instrumentation with MRI. Reliability of developing spontaneous in this model is very high (Bedner et al., 2015).

3.2. ECG recordings

The following parameters were examined from the ECG: QRS amplitude, QRS duration, QT time, RR interval, and RR variability. There were no significant differences between the control and the kainate groups 2 days or 30 days after injection (Table 1).

3.3. Echocardiography

No changes considered to be of biological significance were seen. There was, however, a minor increase in the left ventricle internal dimension during systole (LVIDs)($p = 0.03$) and in interventricular septum thickness through systole (IVSs)($p = 0.046$) in the 30 days post-injection kainate group.

3.4. Histopathology

HE stained sections from the left ventricle of mice 2 days post-injection showed normal myocardial histology both in the kainate group and the control group. Also, in animals sacrificed 30 days after injection, histopathological abnormalities of the myocardium were detected neither in the kainate group nor in the control group (Fig. 3 a,b). Likewise, MSB staining revealed no proliferation of fibrous tissue in any of the groups (Fig. 3 c,d).

3.5. MRI

Tissue phase mapping (TPM) was measured in the long axis and short axis view. In the 30 days post-injection kainate group, the short-axis LV peak strain was 11 % (SD 0.8) compared to 9.1 % (SD 0.4) in the 30 days post-injection sham group ($p \leq 0.005$) (Table 1). There were, however, no significant differences in the other short-axis parameters of

Table 1
MRI, ECG, Echocardiography and histology data.

Parameter	Baseline	2 days post-inj Sham	2 days post-inj Kainate	P Value	30 days post-inj Sham	30 days post-inj Kainate	P Value
MRI Data	**n = 10**	**n = 10**	**n = 13**		**n = 6**	**n = 7**	
***TPM short axis**							
LV Peak Strain	11 (0.9)	9 (1.3)	9 (2.3)	0.9	9.1 (0.4)	11 (0.8)	0.005*
LV Strain rate systole	5 (0.4)	4 (0.7)	5(0.4)	0.6	5 (0.4)	5 (0.4)	0.9
LV Strain rate diastole	5 (0.8)	4 (1.1)	4 (1.1)	0.469	4 (0.9)	5 (0.9)	0.1
RV Peak Strain	7 (1.6)	7 (2.0)	8 (2.9)	0.353	6(1.4)	7 (1.6)	0.4
RV Strain rate systole	4 (0.8)	3 (0.7)	4 (0.6)	0.22	4 (0.7)	4 (0.5)	0.9
RV Strain rate diastole	3 (0.9)	3 (0.5)	4 (0.9)	0.341	3 (0.6)	4 (0.9)	0.9
***TPM long axis**							
LV Peak Strain	8 (1.9)	9 (1.6)	9 (2.0)	0.729	9 (0.8)	10 (0.4)	0.7
LV Strain Systole	4 (0.7)	3 (0.6)	4 (0.5)	0.070	4 (0.4)	4 (0.5)	0.6
LV Strain ED	4 (1.1)	4 (0.8)	4 (0.9)	0.823	5 (0.7)	5 (0.9)	0.4
RV Peak Strain	13 (2.3)	14 (1.8)	15 (1.3)	0.329	14 (2.3)	14 (2.3)	0.9
RV Strain Systole	5 (0.9)	4 (0.6)	5 (0.8)	0.005	5 (0.6)	5 (0.8)	0.1
RV Strain ED	4.5 (0.9)	6 (0.9)	5 (1.0)	0.063	5 (0.9)	5 (0.8)	0.9
***T1 Mapping**	**n = 0**	**n = 0**	**n = 0**	–	n = **6**	**n = 5**	
EVF long axis	N/A	N/A	N/A	N/A	28 % (1.3)	28 % (1.9)	0.9
EVF short axis	N/A	N/A	N/A	N/A	28 % (1.3)	29 % (1.8)	0.4
***CINE**	**n = 10**	**n = 10**	**n = 13**		**n = 6**	**n = 7**	
SV	38 (4)	38 (3.4)	34 (6)	0.15	37 (6)	40 (5)	0.4
CO	21.4 (2.3)	21 (2.3)	19 (3)	0.15	20 (4)	21 (2.3)	0.6
EF	62 (4)	58 (5)	58 (5)	1	61 (5)	61 (2)	0.7
ECG	**n = 24**	**n = 10**	**n = 13**		**n = 6**	**n = 7**	
QRS amp	1710 (470)	1537 (278)	1508 (340)	0.9	1497 (299)	1573 (284)	0.6
QRS duration	8 (0.7)	8 (0.5)	8 (0.68)	0.98	9 (0.9)	8,4 (0.98)	0.9
QT time	51 (1.8)	49 (2)	51 (2)	0.3	49 (3)	49 (3)	1
RR interval	145 (18)	132 (18)	142 (20)	0.5	145 (12)	152 (16)	0.4
HRV	2.3 (1.3)	4 (1)	2.4 (1.4)	0.3	4.2 (3)	5 (5)	0.9
Echocardiography	**n = 24**	**n = 10**	**n = 13**		**n = 6**	**n = 7**	
LVIDd	4.6 (0.2)	4.5 (0.1)	4.4 (0.3)	0.5	4.3 (0.2)	5 (0.3)	0.1
LVIDs	3.8 (0.2)	3.8 (0.1)	3.5 (0.3)	0.3	3.5 (0.2)	4 (0.3)	0.03*
IVSd	0.6 (0.1)	0.7 (0.0)	0.7 (0.0)	0.3	0.7 (0.1)	0.7 (0.1)	0.7
IVSs	0.7 (0.1)	1.0 (0.8)	0.7 (0.4)	0.4	1.2 (0.2)	0.7 (0.1)	0.05*
LVPWd	0.7 (0.1)	0.8 (0.0)	0.7 (0.4)	0.1	0.7 (0.5)	0.7 (0.1)	0.08
LVPWs	0.9 (0.1)	0.9 (0.5)	0.9 (0.7)	0.1	0.9 (0.1)	0.9 (0.1)	0.9
Histology	**n = 0**	**n = 4**	**n = 6**		**n = 6**	**n = 7**	
H&E	N/A	N	N		N	N	
MSB	N/A	N	N		N	N	

Values are presented in means (SD). Significance level is set to $p < 0.05$. All calculations are contrasted with the equivalent control. 2 days post-inj. Sham: animals studied 2 days after intrahipocampal injection with saline water, 2 days post-inj. kainate: animals studied 2 days after intrahipocampal injection with kainate, 30 days post-inj. Sham: animals studied 30 days after intrahipocampal injection with saline water, 30 days post-inj. kainate: animals studied 30 days after intrahipocampal injection with kainate. All MRI TPM Strain rate in cm/sec. TPM: Tissue phase mapping. LV: left ventricle. RV: right ventricle. ED: end of diastole. EVF: extracellular volume fraction (%). SV: stroke volume (μl). CO: cardiac output (ml/min). EF: ejection fraction (%). QRS amplitude (mV), QRS duration (ms), QT time (ms), RR interval (ms), HRV: heart rate variability (ms). LVIDd (mm): left ventricle internal dimension during diastole. LVIDs (mm): left ventricle internal dimension during systole. IVSd (mm): Interventricular septum thickness through diastole. IVSs (mm): Interventricular septum thickness through systole. LVPWd (mm): left ventricle posterior wall thickness through diastole. LVPWs(mm): left ventricle posterior wall thickness through systole. N: Normal.n: number. na: not applicable.

LV strain (LV strain rate in systole, LV strain rate in diastole). Left ventricular long-axis parameters were also not significantly different between the groups. RV strain was not significantly different between the groups. CINE sequence showed a stroke volume (SV) in the 30 days post-injection kainate group of 40 μl compared to 37 μl in the 30 days post-injection sham group ($p = 0.4$). No differences between any of the groups were found in other parameters, such as cardiac output (CO) or ejection fraction (EF).

4. Discussion

Our study is the first one using MRI and the only one combining 4 different diagnostic modalities (MRI, ECG, echocardiography, and histology) for studying structural and functional cardiac remodeling in a murine model of epilepsy. At large, we were not able to detect any changes in cardiac structure or function, neither in 2 days post-injection nor in 30 days post-injection mice. The only MRI parameter showing statistical significance was prolonged short-axis left ventricle strain rate in 30 days post-injection mice, which would have implied increased, not decreased function. Combined with the varying results from echocardiography, the isolated statistical significances observed must be interpreted with great caution and are not considered of any biological relevance.

Our study failed to reproduce the work of Read and collaborators (Table 1). Notably, unlike the Read study, we used cardiac MRI to measure stroke volume, ejection fraction, cardiac output, and deformation parameters. These novel quantitative measurements are all accurate and should be able to detect even small differences in cardiac structure and function (Espe et al., 2017a). In combination with the other three modalities, we consider our study to display a high diagnostic sensitivity, although we are aware of borderline low numbers of animals per group.

The nature of SUDEP poses challenges to the performance of clinical research as it *per definition* strikes without warning. Basic research is conducted using animal experiments, most of which have investigated how far seizures impact on the autonomic nerve system. At large, these studies converge on increased ictal sympathetic and parasympathetic activity and the presence of ictal bradycardia (reviewed in Pansani

et al., 2016).

It is important to keep in mind that animal studies under no circumstances represent genuine SUDEP, as both seizures and death never occur unexpectedly but under controlled conditions. In this sense, a critical point is related to the use of different agents, as both anesthesia and chemoconvulsants could influence physiological parameters and interfere with the experimental results. In all studies completed so far, general anesthesia, predominantly xylazine or medetomidine in combination with ketamine, has been used either to install equipment for electrostimulation or as part of the procedure to provoke seizures. Anesthesia in small rodents is however challenging for several reasons and may be associated with adverse effects on experimental results, especially when the heart is region of interest (Gargiulo et al., 2012). Alpha-2- adrenergic agonists, for example, may have a severe impact on heart rate and function, including bradycardia, bradyarrhythmias, reduction in cardiac output, and hypertension/ hypotension, and may also lead to respiratory depression in combination with other sedative agents (Sinclair, 2003). Particularly the duration of general anesthesia may influence the results as long lasting procedures significantly increase the risk of hypothermia, hypoglycemia, and hypoxia (Zuurbier et al., 2002). To reduce the exposure time to general anesthesia, we treated our mice with the medetomidine antidote atipamezolhydrochloride (300 mg/kg, i.p.) immediately after kainate injection. We also carefully monitored our mice and kept them under optimal conditions, including control of body temperature.

In previous studies, different methods were used to elicit seizures, including amygdala kindling, electroshock application, and systemic use of chemoconvulsants. In all but one study (Read et al., 2015), chemoconvulsants were administered intraperitoneally. In how far intraperitoneal administration may have a direct effect on specific organs, including heart and lung, is speculative. For the chemoconvulsants kainate and pilocarpine, no systematic exploration of cardiac pathology after systemic versus local administration exists. At least one comparative study explores the effect of the kainate analog domoic acid, showing no difference in the observed cardiomyopathies between the intraperitoneal and intrahippocampal groups (Vranyac-Tramoundanas et al., 2011). We aimed at avoiding a potential systemic effect by injecting kainic acid locally above the hippocampus.

Only a few animal studies exist on the relation between acquired epilepsy and signs of damaged cardiac tissue, partly with conflicting results (Pansani et al., 2016). As earlier discussed, these dissimilarities, including the negative results from our experiments, could be explained by the use of different experimental procedures to elicit seizures and different basal conditions under anesthesia. Whereas Read et al. describes increased cardiac collagen deposition already 48 h after chemically induced SE, Naggar et al. could not find any signs of significant cardiac fibrosis after up to 11 months. Both studies were performed in Sprague-Dowley rats, with similar general anesthesia (use of ketamine + xylazine vs. ketamine + medetomidine), and kainate as chemoconvulsant. The only difference was local vs. systemic administration of kainate to elicit SE (Naggar et al., 2014; Read et al., 2015).

It can be discussed whether mouse models are relevant at all for studying the human situation as we even see variable susceptibility to a fibrotic injury between inbred mouse strains with different genetic backgrounds (Walkin et al., 2013). Genetic and phenotypic differences including animal size, heart rate and a range of other characteristics may all influence vulnerability under different natural and experimental conditions. Nonetheless, mice are widely used in the study of cardiac function and structure (Rai et al., 2017), and we know that there are similar responses to cardiac stress in murine and human hearts, as for example, ischemia or increased afterload will both induce cardiac fibrosis. Yet, little is known about the propensity of cardiac stress responses and structural damage due to SE among different animal species or strains of the same species. This illustrates that further research is needed to investigate the influence of epilepsy on cardiac function and structure under variable conditions and in different animal models.

Although our study did not show evidence of myocardial pathology after SE and results from other animal studies have been conflicting, the conclusion that seizure-induced myocardial pathology is unlikely to play a role in SUDEP would have been premature. In postmortem studies of SUDEP victims cardiac pathology including fibrosis and myocyte hypertrophy has been found in approximately 25 % of cases (Nascimento et al., 2017), and it cannot be ruled out that the myocardial pathology in these cases represented an arrhythmogenic substrate playing a part in a terminal seizure induced arrhythmia. However, a recent postmortem study did not find evidence of increased cardiac pathology in SUDEP cases compared with individuals that had died from trauma (Devinsky et al., 2018). Nevertheless, in this study, the majority of cases (10/18) included in the analysis were possible SUDEP implying that they may have died from other causes and as the number of SUDEP cases also was small, these results should be interpreted with caution. Future studies will hopefully increase our understanding of cardiac pathology in the causation of SUDEP.

Ethical publication statement

We confirm that we have read the Journal´s position on issues involved in ethical publication and affirm that this report is consistent with those lines.

Declaration of Competing Interest

Portions of this research have been presented in abstract/poster form at the Norwegian Research School of Neuroscience 2016 and as an oral presentation in Nevrodagene 2017.

This research was partially supported by South-Eastern Norway Regional Health Authority (Helse Sør-Øst RHF) and the The Norwegian Epilepsy Society (Norwegian chapter of the ILAE). The study was also supported by the European Commission (ERA-NET NEURON, BrIE, to KH).

Acknowledgement

We would like to thank Ioanni Veras, for assistance with MRI acquisitions Emil KS Espe for his guidance in MRI analyses, both at the Institute for experimental medical research (IEMR), Oslo University Hospital - Ullevål, Oslo, Norway. Also, thanks to Andy Edwards at Simula Research Center, Oslo, Norway, for his supervision in the analysis of ECGs. We would like to thank Professor Christian Steinhäuser and Ph.D. Peter Bedner from the Institute of Cellular Neurosciences University of Bonn Medical Center for their help in establishing and traineeship on the animal model, consistent advice, and friendship.

References

Ansakorpi, H., Korpelainen, J.T., Suominen, K., Tolonen, U., Myllylä, V.V., Isojärvi, J.I., 2000. Interictal cardiovascular autonomic responses in patients with temporal lobe epilepsy. Epilepsia 41, 42–47.

Ansakorpi, H., Korpelainen, J.T., Huikuri, H.V., Tolonen, U., Myllylä, V.V., Isojärvi, J.I., 2002. Heart rate dynamics in refractory and well controlled temporal lobe epilepsy. J. Neurol. Neurosurg. Psychiatry 72, 26–30.

Auzmendi, J., Buchholz, B., Salguero, J., Cañellas, C., Kelly, J., Men, P., Zubillaga, M., Rossi, A., Merelli, A., Gelpi, R.J., Ramos, A.J., Lazarowski, A., 2018. Pilocarpine-induced status epilepticus is associated with P-Glycoprotein induction in Cardiomyocytes, electrocardiographic changes, and sudden death. Pharmaceuticals Basel 2018, 11.

Bedner, P., Dupper, A., Huttmann, K., Muller, J., Herde, M.K., Dublin, P., Deshpande, T., Schramm, J., Häussler, U., Haas, C.A., Henneberger, C., Theis, M.C., Steinhäuser, C., 2015. Astrocyte uncoupling as a cause of human temporal lobe epilepsy. Brain 138, 1208–1222.

Devinsky, O., 2004. Effects of seizures on autonomic and cardiovascular function. Epilepsy Curr. 4, 43–46.

Devinsky, O., Kim, A., Friedman, D., Bedigian, A., Moffatt, E., Tseng, Z.H., 2018. Incidence of cardiac fibrosis in SUDEP and control cases. Neurology 91, e55–e61.

Earnest, M.P., Thomas, G.E., Eden, R.A., Hossack, K.F., 1992. The sudden unexplained

death syndrome in epilepsy: demographic, clinical, and postmortem features. Epilepsia 33, 310–316.
Espe, E.K.S., Aronsen, J.M., Eriksen, M., Sejersted, O.M., Zhang, L., Sjaastad, I., 2017a. Regional dysfunction after myocardial infarction in rats. Circ. Cardiovasc. Imaging 10 (9). https://doi.org/10.1161/CIRCIMAGING.116.005997. pii: e005997.
Espe, E.K.S., Skårdal, K., Aronsen, J.M., Zhang, L.L., Sjaastad, I., 2017b. A semiautomatic method for rapid segmentation of velocity-encoded myocardial magnetic resonance imaging data. Magn Reso Med. 78, 1199–1207.
Finsen, A.V., Christensen, G., Sjaastad, I., 2005. Echocardiographic parameters discriminating myocardial infarction with pulmonary congestion from myocardial infarction without congestion in the mouse. J. Appl. Physiol. 98, 680–689.
Gargiulo, S., Greco, A., Gramanzini, M., Esposito, S., Affuso, A., Brunetti, A., Vesce, G., 2012. Mice anesthesia, analgesia, and care, Part II: anesthetic considerations in preclinical imaging studies. ILAR J. 53, E70–81.
Glasscock, E., Yoo, J.W., Chen, T.T., Klassen, T.L., Noebels, J.L., 2010. Kv1.1 potassium channel deficiency reveals brain-driven cardiac dysfunction as a candidate mechanism for sudden unexplained death in epilepsy. J. Neurosci. 30, 5167–5175.
Harden, C., Tomson, T., Gloss, D., Buchhalter, J., Cross, J.H., Donner, E., French, J.A., Gil-Nagel, A., Hesdorffer, D.C., Smithson, W.H., Spitz, M.C., Walczak, T.S., Sander, J.W., Ryvlin, P., 2017. Practice guideline summary: Sudden unexpected death in epilepsy incidence rates and risk factors: Report of the Guideline Development, Dissemination, and Implementation Subcommittee of the American Academy of Neurology and the American Epilepsy Society. Neurology 26, 1674–1680.
Isojärvi, J.I., Ansakorpi, H., Suominen, K., Tolonen, U., Repo, M., Myllylä, V.V., 1998. Interictal cardiovascular autonomic responses in patients with epilepsy. Epilepsia 39, 420–426.
Istrătoaie, O., OfiŢeru, A.M., Nicola, G.C., Radu, R.I., Florescu, C., Mogoantă, L., Streba, C.T., 2015. Myocardial interstitial fibrosis - histological and immunohistochemical aspects. Rom. J. Morphol. Embryol. 56, 1473–1480.
Krenning, G., Zeisberg, E.M., Kalluri, R., 2010. The origin of fibroblasts and mechanism of cardiac fibrosis. J. Cell. Physiol. 225, 631–637.
Mueller, S.G., Bateman, L.M., Laxer, K.D., 2014. Evidence for brainstem network disruption in temporal lobe epilepsy and sudden unexplained death in epilepsy. Neuroimage Clin. 5, 208–216.
Myers, K.A., Sivathamboo, S., Perucca, P., 2018. Heart rate variability measurement in epilepsy: How can we move from research to clinical practice? Epilepsia 59, 2169–2178.
Naggar, I., Lazar, J., Kamran, H., Orman, R., Stewart, M., 2014. Relation of autonomic and cardiac abnormalities to ventricular fibrillation in a rat model of epilepsy. Epilepsy Res. 108, 44–56.
Nascimento, F.A., Tseng, Z.H., Palmiere, C., Maleszewski, J.J., Shiomi, T., McCrillis, A., Devinsky, O., 2017. Pulmonary and cardiac pathology in sudden unexpected death in epilepsy (SUDEP). Epilepsy Behav. 7, 119–125.
Nashef, L., Walker, F., Allen, P., Sander, J.W., Shorvon, S.D., Fish, D.R., 1996. Apnoea and bradycardia during epileptic seizures: relation to sudden death in epilepsy. J. Neurol. Neurosurg Psychiatry 60, 297–300.
Nashef, L., So, E.L., Ryvlin, P., Tomson, T., 2012. Unifying the definitions of sudden unexpected death in epilepsy. Epilepsia 53, 227–233.
Natelson, B.H., Suarez, R.V., Terrence, C.F., Turizo, R., 1998. Patients with epilepsy who die suddenly have cardiac disease. Arch. Neurol. 55, 857–860.
Noebels, J.L., 2017. Precision physiology and rescue of brain ion channel disorders. J. Gen. Physiol. 149, 533–546.
Pansani, A.P., Colugnati, D.B., Scorza, C.A., de Almeida, A.C., Cavalheiro, E.A., Scorza, F.A., 2016. Furthering our understanding of SUDEP: the role of animal models. Exp. Rev. Neurother. 16, 561–572.
P-Codrea Tigaran, S., Dalager-Pedersen, S., Baandrup, U., Dam, M., Vesterby-Charles, A., 2005. Sudden unexpected death in epilepsy: is death by seizures a cardiac disease? Am. J. Forensic Med. Pathol. 26, 99–105.
Rai, V., Sharma, P., Agrawal, S., Agrawal, D.K., 2017. Relevance of mouse models of cardiac fibrosis and hypertrophy in cardiac research. Mol. Cell Biochem. 424 (January), 123–145.
Read, M.I., McCann, D.M., Millen, R.N., Harrison, J.C., Kerr, D.S., Sammut, I.A., 2015. Progressive development of cardiomyopathy following altered autonomic activity in status epilepticus. Am. J. Physiol-Heart Circ. Physiol. 309, H1554–64.
Sadredini, M., Danielsen, T.K., Aronsen, J.M., Manotheepan, R., Hougen, K., Sjaastad, I., Stokke, M.K., 2016. Beta-adrenoceptor stimulation reveals Ca2+ waves and sarcoplasmic reticulum Ca2+ depletion in left ventricular cardiomyocytes from post-infarction rats with and without heart failure. PLoS One 11, e0153887.
Saetre, E., Abdelnoor, M., 2018. Incidence rate of sudden death in epilepsy: a systematic review and meta-analysis. Epilepsy Behav. 86, 93–199.
Sinclair, M.D., 2003. A review of the physiological effects of alpha2-agonists related to the clinical use of medetomidine in small animal practice. Can. Vet. J. 44, 885–897.
Suorsa, E., Korpelainen, J.T., Ansakorpi, H., Huikuri, H.V., Suorsa, V., Myllylä, V.V., Isojärvi, J.I., 2011. Heart rate dynamics in temporal lobe epilepsy-A long-term follow-up study. Epilepsy Res. 93, 80–83.
Tinuper, P., Bisulli, F., Cerullo, A., Carcangiu, R., Marini, C., Pierangeli, G., Cortelli, P., 2001. Ictal bradycardia in partial epileptic seizures: autonomic investigation in three cases and literature review. Brain 124, 2361–2371.
Vranyac-Tramoundanas, A., Harrison, J.C., Sawant, P.M., Kerr, D.S., Sammut, I.A., 2011. Ischemic cardiomyopathy following seizure induction by domoic Acid. Am. J. Pathol. 179, 141–154.
Walkin, L., Herrick, S.E., Summers, A., Brenchley, P.E., Hoff, C.M., Korstanje, R., Margetts, P.J., 2013. The role of mouse strain differences in the susceptibility to fibrosis: a systematic review. Fibrogenesis Tissue Repair 6, 18.
Walton, N.Y., Rubinstein, B.K., Treiman, D.M., 1995. Cardiac hypertrophy secondary to status epilepticus in the rat. Epilepsy Res. 20, 121–124.
Zuurbier, C.J., Emons, V.M., Ince, C., 2002. Hemodynamics of anesthetized ventilated mouse models: aspects of anesthetics, fluid support, and strain. Am. J. Physiol. Heart Circ. Physiol. 282, H2099–105.